THE EFFECT OF CHANGED MASS RATIO ON THE MOTION OF A TETHERED CYLINDER

K. Ryan
M. C. Thompson
and K. Hourigan
Fluids Laboratory for Aeronautical and Industrial Research (FLAIR),
Department of Mechanical Engineering,
Monash University, Melbourne, Victoria 3800, Australia

Abstract

The flow past a buoyant tethered cylinder is investigated for a variety of mass ratios. A critical mass ratio, $m^* = 0.2 - 0.3$ has been found for the uniform flow past a tethered cylinder, below which sustained large amplitude oscillations are observed up to the highest reduced velocity simulated in this study. The critical mass ratio is found to coincide closely with that found for a hydro-elastically mounted cylinder using two-dimensional simulations in previous studies.

1.   Introduction

To date, few studies on the uniform flow past a tethered body exist, most of these concentrating on the flow past a tethered sphere. This is despite tethered cylinders having practical applications in subsea pipelines, tethered lighter-than-air-craft, and tethered spars just to name a few examples.

A significant body of research exists in the related field of freely oscillating cylinders, both with high- and low- mass damping. For both cases, several parameter studies have been performed, including studies regarding the effect of mass ratio on the modes of oscillation observed. In particular, Govardhan and Williamson, 2000 observed that for low mass damped hydro-elastically mounted cylinders three modes of oscillation exist, namely the initial, upper and lower branch, and a critical mass ratio exists below which high amplitude oscillations continue up to an indefinite reduced velocity. Recent studies by Govardhan and

1

Williamson, 2003 have confirmed that this phenomenon occurs up to an infinite reduced velocity.

Three phenomena distinguish the tethered cylinder from the hydro-elastically mounted cylinder. The first is that the cylinder now has a component of motion in both the in-line and transverse directions, and as such variations in both the drag and lift forces directly affect the cylinder motion.

Secondly, the natural frequency of the cylinder system (expressed in non-dimensional form as the reduced velocity) is now a function of the hydro-dynamic loading acting on the cylinder, and varies with lift and drag throughout the oscillation cycle through the equation:

$$U^* = \frac{U}{f_n D} = \sqrt{\frac{\pi(m^* + C_A)L^*}{2\sqrt{C_D^2 + \left[C_L + \frac{\pi}{2}\frac{(1-m^*)}{Fr^2}\right]^2}}} \qquad (1)$$

Where C_D is the drag coefficient, C_L is the lift coefficient, m^* is the mass ratio, Fr is the Froude number, L^* is the tether length normalized by the cylinder diameter, and C_A is the added mass coefficient, equal to unity for a circular cylinder.

At very high Froude numbers, (corresponding experimentally to high velocities), assuming a fixed mean drag and lift the dependance on the fluid forces and Froude number impose an upper limit on the possible maximum value for the reduced velocity. From equation 1, in order to exceed this maximum value the absolute value of either the mean drag and/or the mean lift must decrease.

The third distinguishing feature is that there is no damping (it is assumed that the tether attachment point is frictionless) with the direct result that, assuming the forcing and resultant cylinder motion are well approximated by a sinusoidal function, there can be no 'upper' branch as described by Govardhan and Williamson, 2000. The phase angle between the total force and the cylinder motion, and the phase angle between the vortex force and the cylinder motion, must both be 180° for significant oscillation amplitudes.

There are two solutions of importance as the flow conditions are varied, namely the mean layover angle, θ, and the cylinder oscillations about this mean layover angle, θ^*_{std}.

To date, only the two-dimensional studies of Pregnalato et al., 2002, Ryan et al., 2002 and Ryan et al., 2003 have reported studies on the flow past a tethered cylinder. In these related papers, only one cylinder mass ratio and tether length ratio was studied ($m^* = 0.833, l^* = 5.05$), however, at large layover angles, θ (where the tethered cylinder experiences dominantly transverse oscillations), oscillations similar to that of

a freely oscillating cylinder were reported, and it may be assumed that a tethered cylinder may have a critical mass ratio similar to that found for a freely oscillating cylinder.

In this paper two-dimensional simulations of a tethered cylinder with various mass ratios ($m^* = 0.1 - 0.8$) and a tether length, $l^* = 5$, are reported (see Figure 1a.). The reduced velocity: was chosen as the controlling flow parameter. All simulations were performed at a Reynolds number, $Re = 200$. Simulations were carried out with a highly accurate spectral element method coupled with a predictor corrector technique, details of which may be found in Pregnalato et al., 2002.

2.   Numerical Method

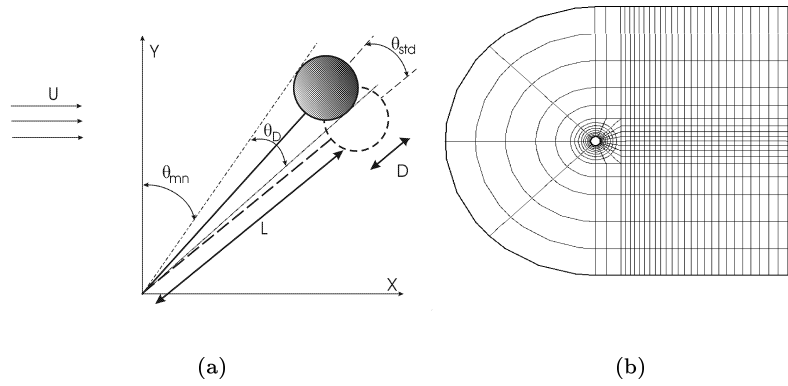(a)   (b)

Figure 1.   Schematic of the tethered cylinder system (a), and the computational grid used for the calculations (b)

The fluid forces acting on the tethered cylinder may be decomposed into the drag force acting in-line with the fluid flow, the lift force and the buoyancy force, both acting transverse to the fluid flow, a restoring tension force (T) in the tether is also present.

The problem is fully described in two dimensions by the coupled system of the incompressible Navier-Stokes equations (equations 2a and 2b) and the equations of motion describing the body acceleration in response to calculated fluid forces (equations 3a and 3b). The two-dimensional form of the the Navier Stokes equations is written as:

$$\frac{\partial \mathbf{u}}{\partial t} + (\mathbf{u} \bullet \nabla)\mathbf{u} \quad = \quad -\frac{1}{\rho_f}\nabla p + \frac{1}{Re}\nabla^2 \mathbf{u}, \qquad (2a)$$

$$\nabla \bullet \mathbf{u} \quad = \quad 0, \qquad (2b)$$

4

where **u** is the velocity field, p is the pressure field, ρ_f is the density of the fluid, and Re is the flow Reynolds number.

The equations governing the cylinders motion (here presented in cartesian coordinates) are:

$$\ddot{x} = \frac{\gamma}{l^2 m^*}\left[\left(l^2 - x^2\right)C_D - x\left(y\left[C_L + \frac{\pi}{2}(1-m^*)\frac{1}{Fr^2}\right]\right)\right] \quad (3a)$$

$$\ddot{y} = \frac{\gamma}{l^2 m^*}\left[\left(l^2 - y^2\right)\left(C_L + \frac{\pi}{2}(1-m^*)\frac{1}{Fr^2}\right) - yxC_D\right] \quad (3b)$$

where l is the tether length and $\gamma = \frac{2U^2}{\pi D}$. Note that γ is dimensional and has units of acceleration.

The (two-dimensional) spectral-element mesh used in this study is shown in Figure. 1b. It consists of K = 518 macro elements. A comprehensive resolution study was performed for a stationary cylinder at a Reynolds number, Re = 500 (based on cylinder diameter), and also for a tethered (moving) cylinder at a Reynolds number, Re = 200. For each study, the order of the interpolating polynomials was increased from N = 5 to N = 9 to test for grid resolution. The variation in shedding frequency, lift and drag between the values at N = 7 and N = 9 are less than 1%. Furthermore, for the fixed cylinder, the values of all measures for N = 8 (used in all simulations) compare to within 1% of the numerical values of Blackburn and Henderson, 1999 and Henderson, 1995.

3.   Results

The results are divided into the mean results (mean layover angle and drag coefficient) and the amplitude of oscillations about this mean layover angle. Variations in the mean results indicate changes in the wake structure and have been found to be directly linked to changes in the oscillatory results.

Two oscillation modes have been identified for mass ratios $m^* < 0.3$. The switch between the two wake types is identified by a discontinuous jump in the mean layover angle and the mean hydrodynamic forces acting on the cylinder, and a discontinuous jump in the cylinder oscillation amplitude.

3.1   Mean Layover Results

Figure. 2 shows the mean layover angle (θ_{mn}) as a function of reduced velocity, for each of the mass ratios investigated. In general the rate of change of mean layover angle (as a function of increasing reduced velocity) varies inversely with the mass ratio. For mass ratios, $m^* =$
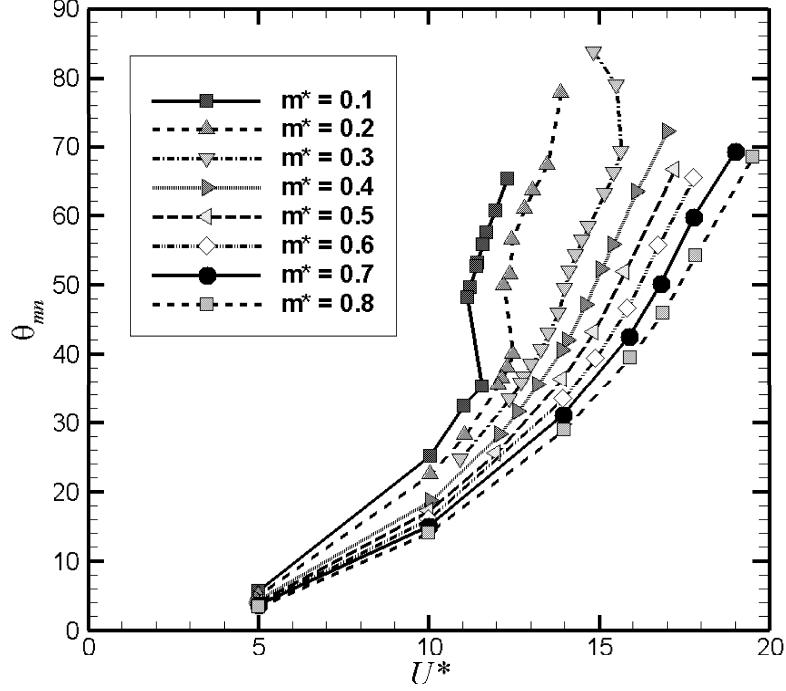
Figure 2. Mean layover angle θ_{mn} as a function of the reduced velocity U^*

$0.3 - 0.8$, the variation in mean layover angle is a smooth function of the reduced velocity. However, for $m^* = 0.1$ and 0.2 a distinct jump in the mean layover angle is observed in the range $\theta_{mn} = 40 - 50^o$. A very small reduced velocity range (the transition range) is observed for $m^* = 0.1$ and 0.2 where one of two mean layover angles is possible for a given value of U^*.

The mean layover angle can be determined explicitly by equating the mean fluid forces acting on the cylinder:

$$\theta_{mn} = Tan^{-1} \left[\frac{C_D}{C_L + \frac{(1-m^*)\pi}{Fr^2}} \right]. \qquad (4)$$

As the Froude number varies smoothly with the reduced velocity (equation. 1), equation. 4 shows that the discontinuous jump in the

mean layover angle must be associated with a discontinuous increase in the mean drag and/or a discontinuous decrease in the mean lift.

The discontinuous change in the absolute value of the mean drag and/or lift may account for the reduced velocity transition region (which from equation. 1 is a function of both of these parameters).
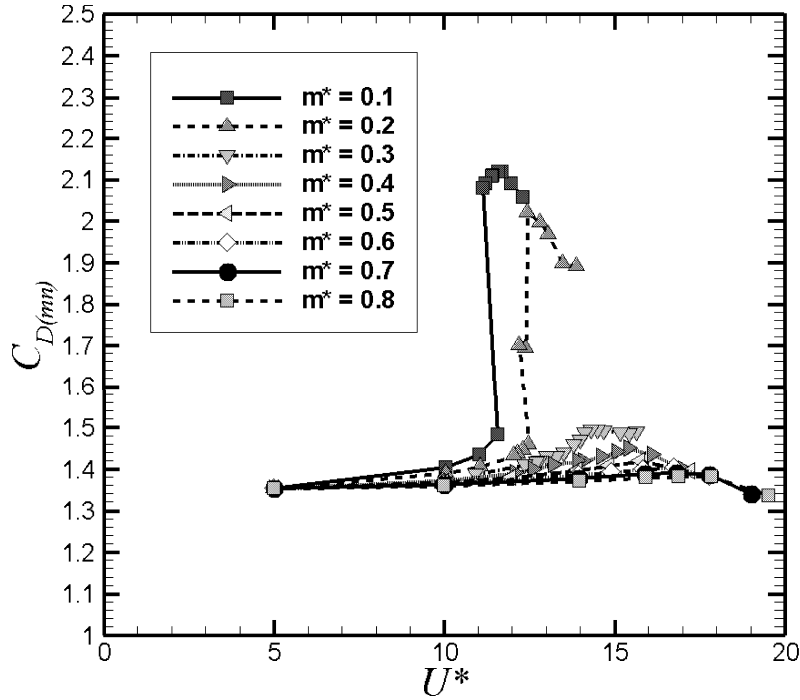
3.2   Mean Drag Results

Figure 3.   Mean drag $C_{D(mn)}$ as a function of the reduced velocity U^*

The mean drag is plotted as a function of the reduced velocity in figure. 3. As anticipated, a significant increase in the mean drag is observed for mass ratios, $m^* = 0.1$ and 0.2 corresponding to the discontinuous jump in the mean layover angle. For all the mass ratios investigated the mean drag reached a maximum value prior to decreasing. In the case of $m^* = 0.8$ and 0.9 the mean drag is observed to decrease below that for a fixed cylinder at this Reynolds number ($C_D < 1.34$). This is

a direct result of the limiting reduced velocity which may be predicted from equation. 1.
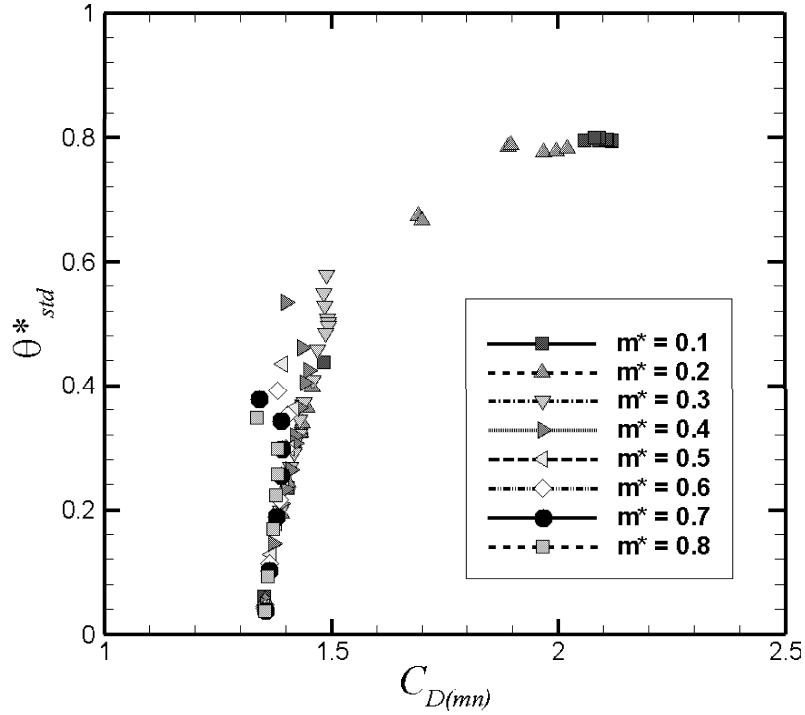

Figure 4. Mean drag $C_{D(mn)}$ as a function of the normalized amplitude of oscillation θ^*_{std}

Given the dramatic increase in the mean drag observed for $m^* = 0.1, 0.2$ it may be assumed that the wake dynamics have significantly altered, and more specifically that the amplitude of oscillation has also increased. Figure. 4 shows the amplitude of oscillation, θ^*_{std} as a function of the mean drag, $C_{D(mn)}$. The oscillation amplitude is defined as the standard deviation of the cylinder's motion normalized by the angle subtended by the cylinder diameter, D. (see figure. 1a). For $m^* = 0.1, 0.2$ the increase in drag is observed to be directly related to an increase in the amplitude of cylinder oscillation. For higher mass ratios there is no jump away from a mean drag range, $C_D = 1.3 - 1.6$ and no jump in the oscillation amplitude.

It appears from the above results that there are two distinct states for the cylinder for $m^* < 0.3$. A state of low amplitude oscillation and low mean drag, and a state of high amplitude oscillation and high mean drag. The transition between the two states involves a dramatic increase in the mean layover angle. The high amplitude state is not observed for higher mass ratios. The amplitude of oscillation for the high amplitude state appears remarkably constant for both $m^* = 0.1$ and 0.2 at a value of $\theta^*_{std} \simeq 0.8$, note that this does not imply that the cylinder is oscillating with an amplitude of 0.8 diameters.
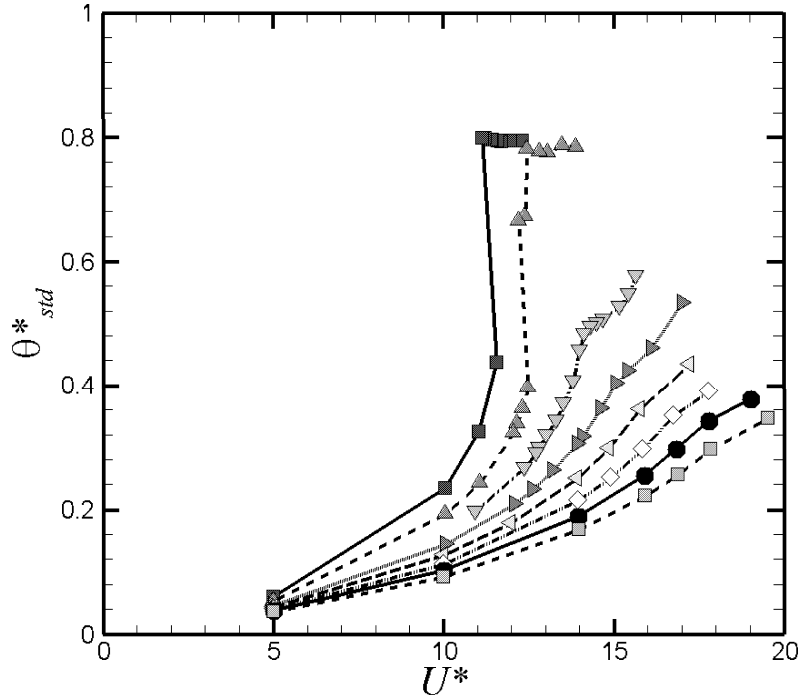
3.3   Cylinder Oscillation Results

Figure 5.   Normalized amplitude of oscillation θ^*_{std} as a function of the reduced velocity U^*

The normalized cylinder amplitude, θ^*_{std} is plotted against the reduced velocity in figure. 5. Here the constant amplitude of the high amplitude state (for $m^* = 0.1, 0.2$) is clearly observed. A slight flattening of the

θ^*_{std}/U^* curve is noticed for a mass ratio, $m^* = 0.3$, however it is believed that this deviation is not the high amplitude state observed for lower mass ratios, as the amplitude of oscillation continues to increase at higher reduced velocities, and the amplitude in this range is not the same as observed for $m^* = 0.1$ and 0.2.

The range of reduced velocity possible is inversely proportional to the mass ratio, such that cylinders with a higher mass ratio have a far more extensive reduced velocity range. With this in mind, the high amplitude state observed for $m^* = 0.1$ and 0.2 extends over a considerable range of the possible U^* values. The work of Ryan et al., 2003 for a cylinder mass ratio $m^* = 0.833$ indicates that for high mass ratios the amplitude of oscillation quickly decreases beyond a maximum value (for $U^* > 21$ in their study). In our study, for the $m^* = 0.1$ and 0.2 case, the reduced velocity range is restricted such that it is believed that the high amplitude state will continue up to the highest reduced velocity possible.

4. Discussion - The existence of a critical mass ratio

The present findings indicate a critical mass ratio, m^*_{crit} between 0.2 and 0.3. For $m^* < m^*_{crit}$ it is possible for the cylinder to oscillate in the high amplitude state. This result compares favorably with the findings of Govardhan and Williamson, 2000 and Govardhan and Williamson, 2003 in their investigations of a low mass-damped cylinder allowed to oscillate freely in a direction transverse to the free-stream. They found that for a $m^* < m^*_{crit}$ high amplitude oscillations resulted. Our present value of m^*_{crit} appears to be considerably less than their critical value (their findings indicating $m^*_{crit} = 0.54$). However in Govardhan and Williamson, 2003 the authors reinterpreted the low Reynolds number, two-dimensional numerical results of Shiels et al., 2001 and found $m^*_{crit} = 0.25$ for this case. This result appears to compare well with the present findings, and as such it may be possible to compare the present results to the freely oscillating cylinder case. However in order to compare our results directly, the nature of the vortex structures in the high amplitude state have to be analyzed in depth which is the subject of a future paper.

5. Conclusion

A critical mass ratio, $m^* = 0.2 - 0.3$ has been found for the uniform flow past a tethered cylinder, below which sustained large amplitude oscillations are observed up to the highest reduced velocity simulated in this study. The critical mass ratio is found to coincide closely with that found for a hydro-elastically mounted cylinder using two-dimensional

simulations in previous studies. However, for a tethered cylinder, the critical mass ratio affects both the mean layover angle as well as the amplitude of oscillation.

Acknowledgments

References

Blackburn, H. M. and Henderson, R. D. (1999). A study of two-dimensional flow past an oscillating cylinder. *Journal of Fluid Mechanics.*, 385:255–286.

Govardhan, R. and Williamson, C. (2000). Modes of vortex formation and frequency response of a freely vibrating cylinder. *Journal of Fluid Mechanics.*, 420:85–130.

Govardhan, R. and Williamson, C. (2003). Resonance forever: existence of a critical mass and an infinite regime of resonance in votex-induced vibration. *Journal of Fluid Mechanics.*, 473:147–166.

Henderson, R. (1995). Details of the drag curve near the onset of vortex shedding. *Physics of Fluids*, 7:2102–2104.

Pregnalato, C., Ryan, K., Thompson, M., and Hourigan, K. (2002). Numerical simulations of the flow-induced vibrations of tethered bluff bodies. In *Proceedings of IMECE 2002: 5th International Symposium on FSI, AE, FIV and N.*

Ryan, K., Pregnalato, C., Thompson, M., and Hourigan, K. (2003). Flow-induced vibrations of a tethered circular cylinder. *Journal of Fluids and Structures.*

Ryan, K., Thompson, M., and Hourigan, K. (2002). Energy transfer in a vortex induced vibrating tethered cylinder system. In *Conference on Bluff Body Wakes and Vortex-Induced vibrations, BBVIV3.*

Shiels, D., Leonard, A., and Roshko, A. (2001). Flow-induced vibration of a circualr cylinder at limiting structural parameters. *Journal of Fluids and Structures*, 15:3–21.